A.V. DVORNICHENKO

Sumy State University
(2, Rimskogo-Korsakova Str., Sumy 40007, Ukraine; e-mail: alina.dvorni4enko@ukr.net)

ELECTROMIGRATION EFFECTS AT EPITAXIAL GROWTH OF THIN FILMS: PHASE-FIELD MODELING

The epitaxial growth of thin films with regard for the anisotropy of the adsorbate surface diffusion induced by electromigration effects has been studied theoretically in the framework of the phase-field theory and with the use of numerical simulations. The influence of the coefficient of electromigration-induced anisotropic diffusion, which is proportional to the applied electric field strength, on the dynamics of growth of the film thickness and the height of surface structures, growing surface morphology, statistical characteristics of the surface multilayer adsorbate structures, and distribution of surface structures over their heights is revealed.

K e y w o r d s: phase-field method, epitaxial growth, surface structures, electromigration, numerical simulation, statistical characteristics.

1. Introduction

The formation of surface structures at elevated temperatures is a result of the self-organization of adsorbed atoms. It is usually driven by such kinetic factors as the rates of processes running at the growing surface. One of the interesting phenomena that affect the formation of a surface morphology at high temperatures is the electromigration, which emerges, when an electric current passes through the substrate [1, 2].

The electromigration is the transport of a material caused by an electric field. This phenomenon comprises an important technological problem, especially concerning the reliability of electronic circuits, which are widely used in modern micro- and nanoelectronics. Atoms move in solids due to diffusion processes and under the action of the electron wind force. The latter arises owing to the momentum transfer from conduction electrons that are scattered at ions in the solid bulk and push those ions along the electron flow direction. The presence of a driving force makes the diffusion process in a material anisotropic and directed along the force direction. As a result, there appears a net atomic flow in this direction.

The overwhelming majority of researches devoted to the electromigration were begun in the 1970s. Mostly, these were experimental studies. It was shown that an electric current, when passing through a substrate, effectively heats its surface and, as a result, the induced spatially oriented drift of adatoms begins to play a substantial role in the formation of surface structures at deposition [3–6]. A reorganization of the step-like structure of adsorbate islands was observed on silicon substrates [7, 8]. The strong electromigration effects manifested themselves in the processes of the vanadium surface morphology evolution [9] and the epitaxial growth of semiconductor heterostructures [10]. It was found that the surface structures grow according to the Stransky–Krastanov mode at low deposition temperatures [11–14]. At the same time, at elevated temperatures, such processes are associated with dewetting of the deposited material layers [15, 16]. Thus, the electromigration effects induced by a potential difference applied to the opposite substrate sides can substantially influence the dynamics of the surface morphology evolution at elevated temperatures. This effect can result in a modification of the coating morphology in comparison with the isotropic case of deposition obtained in the absence of the external field.

The processes of formation and growth of multilayer adsorbate structures during the epitaxial growth of thin films were also analyzed theoretically using a number of methods in the framework of the multiscale modeling scheme (see, e.g., work [17]). This approach makes it possible to qualitatively describe the

processes running at the atomic level [18] with the help of the diffusion time scale [19] and the processes of step-structure formation [20]. It also allows us to study the dynamics of surface morphology changes [21, 22].

When describing the dynamics of surface morphology changes at the mesoscopic level, approaches based on the phase-field theory are widely applied. This method was first proposed in work [23] to simulate the epitaxial growth dynamics of adsorbate islands. Later, it was developed in work [24]. A further generalization of this approach made it possible to study the influence of the adsorbate surface flow fluctuations and the local changes of the surface temperature induced by the adsorption/desorption processes on the surface growth dynamics and surface morphology.

The influence of such parameters as the deposition flux, energy of interaction of an adsorbate with the substrate, and relaxation time of a surface temperature on the statistical parameters of the growing surface and surface structures was studied in work [25]. However, the cited study was performed assuming the isotropic surface diffusion of an adsorbate. Theoretical researches of electromigration effects at the deposition were mainly carried out by considering the interaction between the applied electric field and the effective charge of surface atoms [26–29].

In this work, we will develop the phase-field method to describe the epitaxial formation and growth of multilayer adsorbate surface structures taking the electromigration effects into account. At numerical simulations, the effects of directed adatom drift are involved by introducing anisotropic surface diffusion of adsorbate. The influence of the induced diffusion coefficient on the growth dynamics, morphology, and statistical properties of the surface will be analyzed.

The structure of the work is as follows. A mathematical model describing the evolution of the adsorbate concentration and the surface height, which is based on the phase-field method, is developed in Section 2. Section 3 contains information about the details of a numerical simulation procedure. In Section 4, the simulation results are discussed. The final section contains the main conclusions of the work.

2. Mathematical Model

Let us consider the evolution of a dimensionless adsorbate concentration x on the substrate. The param-

eter x is defined as the ratio between the number of adsorbed atoms (adatoms) N_a and the total number of adsorption sites N_s in each unit cell with the size ℓ; i.e. $x = N_a/N_s$, so that $x \in [0, 1]$. Only the homoepitaxial processes are taken into account, i.e. when the chemical composition of the deposited substance does not differ from that of the substrate. The consideration is carried out in the framework of the phase-field theory.

The space-time evolution of the adsorbate concentration during the epitaxial growth is described by an equation of the reaction-diffusion type. In the standard form, it looks like

$$\partial_t x = R(x) - \nabla \mathbf{J}. \qquad (1)$$

Here, the first term on the right-hand side corresponds to the reaction component. It is determined by the processes that take place at the surface in the course of deposition. The second term describes the surface adsorbate flux.

Among the main reaction processes, the adsorption and desorption are distinguished as a rule. In the course of epitaxial growth, adatoms are deposited at a certain rate k_a, which is proportional to the deposition flux. The adsorbed atoms can be desorbed back to the gas phase at the rate k_{d0}, which is determined in terms of the effective adatom lifetime τ_d and the desorption activation energy E_{des} by the formula

$$k_{d0} = \frac{1}{\tau_d} \exp\left(-\frac{E_{\text{des}}}{T}\right),$$

where T is the deposition temperature expressed in energy units. Since adatoms are mobile interacting particles, the adatom-adatom interaction can modify the desorption rate, $k_d = k_{d0} \exp(U/T)$, where $U(\mathbf{r})$ is the interaction potential between the adsorbate atoms.

The total surface flux of adsorbate, $\mathbf{J}$, includes the ordinary diffusion flux $(-D\nabla x)$ and the flux associated with the interaction potential $U(\mathbf{r})$. The latter determines the thermodynamic force $\mathbf{f} = -\nabla(U/T)$ that acts on the adsorbed particles and induces the flux $\mathbf{v}x$ of adatoms. The velocity $\mathbf{v}$ is determined in the standard way from the Einstein ratio $\mathbf{v} = D\mathbf{f}$. The flux induced by the interaction between the adsorbates is possible only to $(1 - x)$ free sites. The surface diffusion coefficient D is determined in the standard way: $D = a^2\nu \exp(-E_{\text{diff}}/T)$, where a is

the substrate lattice parameter, ν the frequency factor, and E_{diff} the diffusion activation energy ($E_{\text{diff}} >> E_{\text{des}}$).

In order to find an expression for the interaction potential between the adatoms, $U(\mathbf{r})$, let us apply the self-consistent approach. Then, $U(\mathbf{r})$ is a function of the binary attraction potential between two adsorbed particles $u(\mathbf{r})$ and is written in the form

$$U(x(\mathbf{r})) = -\int u(\mathbf{r} - \mathbf{r}')x(\mathbf{r}')d\mathbf{r}'.$$

A similar approach was widely used in theoretical studies of the epitaxial growth processes [25, 30, 31], spatial ordering taking place in the course of surface structuring at the condensation [32–34], radiation-induced defect structuring [35, 36], and so forth. In the framework of this approach, the adsorbate-adsorbate interaction energy ϵ is determined by the integral $\epsilon = \int u(\mathbf{r})d\mathbf{r}$. Then, the first approximation for the interaction potential U brings about the formula $U(x(r)) \simeq -\epsilon x(r)$.

Ultimately, using the obtained expression for the adsorbate-adsorbate interaction potential and combining the reaction and diffusion components, we transform Eq. (1) for the space-time evolution of the adsorbate concentration into the form

$$\frac{\partial x}{\partial t} = F - xe^{-\varepsilon x} + D_0 \left[\nabla^2 x - \varepsilon \nabla M(x)\nabla x\right]. \tag{2}$$

Here, the dimensionless time t is measured in k_{d0}-units, and the dimensionless parameters $F = k_a/k_{d0}$, $D_0 = D/k_{d0}$ and $\varepsilon = \epsilon/T$, as well as the notation $M(x) = x(1 - x)$, are introduced. From Eq. (2), one can see that the flux induced by the adsorbate-adsorbate interaction is directed opposite to the ordinary diffusion flux.

When studying the surface growth processes in the framework of the phase-field theory, the surface height at a definite substrate point and at every time moment is determined by the value of the phase field $\phi(\mathbf{r}, t)$, which is the effective order parameter [24]. The surface height is measured in the units of the lattice parameter a and corresponds to the number of monolayers. Following works [23, 24], the equation of space-time evolution for the phase field ϕ is written in the form

$$\frac{\partial \phi}{\partial t} = -\frac{\delta \mathcal{H}}{\delta \phi}, \tag{3}$$

where the free energy

$$\mathcal{H} = \int d\mathbf{r}[\varpi^2(\nabla\phi)^2/2 + H(\phi, x)] \tag{4}$$

is determined through the density H, and the parameter ϖ is the dimensionless coupling constant.

While describing the growth of multilayer adsorbate structures with terraces, let us assume, following the results of work [23], that the local stable minima of the order parameter correspond to the terraces in the pyramidal structures, whereas the rapid spatial change of the order parameter determines the position of a step in this structure. To model the process of formation of a large number of terraces in the adsorbate structures, we use the following expression for the free energy density [30]:

$$H(\phi, x) = \frac{1}{2\pi}\cos(2\pi[\phi - \phi_s]) -$$
$$- \lambda x\left(\phi + \frac{1}{2\pi}\sin(2\pi[\phi - \phi_s])\right), \tag{5}$$

where the parameter λ determines the terrace width, and the parameter ϕ_s corresponds to the initial surface height. Hence, the dynamics of adsorbate structuring at the epitaxial growth is described by the system of equations (2) and (3) taking Eqs. (4) and (5) into account.

The main aim of this work is to reveal the influence of electromigration effects, which emerge, when an external electric field is applied to the substrate, on the dynamics of surface growth at the deposition, as well as the surface morphology and its statistical characteristics. The application of an electric field to the substrate, when the field direction is parallel to the substrate surface, induces variations in the internal local electric field, which can bring about the appearance of a directed force $\mathbf{F}_{\text{el}} = eZ\mathbf{E}$, where e is the electron charge. The magnitude of the field strength $|\mathbf{E}| = -\Phi/L$ is determined by the potential difference Φ across the substrate and the linear substrate size L (the distance between the anode and cathode). The direction of the force vector $\mathbf{F}_{\text{el}}$ is given by the effective valence Z, which is negative for most metals, so that the adsorbed atoms move in the opposite direction to the electric field.

In order to take the electromigration effects into account, when carrying out a numerical simulation, let us assume that the surface diffusion of adatoms

can be generalized by considering the directed motion of adatoms with the diffusion coefficient D_{em} in one of the directions induced by the electric field. The simplest case of such anisotropic diffusion in the case where the electric field is directed along the direction x is described by the expression $\pm D_{em}\nabla_x x(\mathbf{r})$, where the sign $\pm$ is determined by the relative arrangement of the cathode and anode. Thus, the general system of dynamic equations for the adsorbate concentration $x(\mathbf{r}, t)$ and the phase field $\phi(\mathbf{r}, t)$, which describes the epitaxial growth of a pyramidal adsorbate structures with the electromigration effects, reads

$$\frac{\partial x}{\partial t} = F - xe^{-\varepsilon x} +$$
$$+ D_0 \nabla \mathcal{M}(x)\nabla x + D_{em}\nabla_x x - \frac{1}{2}\frac{\partial \phi}{\partial t}, \qquad (6a)$$
$$\frac{\partial \phi}{\partial t} = \varpi^2 \Delta \phi + \sin(\pi\phi) + \lambda x(1 + \cos(\pi\phi)), \qquad (6b)$$

where the notation $\mathcal{M}(x) = 1 - \varepsilon M(x)$ is used, and, for simplicity, it is put that $\phi_s = 0$. The last term on the right-hand side of Eq. (6a) describes the dynamics of the adsorbate concentration on the growing layer. The component $1 + \cos(\pi\phi)$ on the right-hand side of Eq. (6b) means that the minima of the free energy $\mathcal{H}$ take place at $\phi = 2n + 1$ irrespective of the adatom concentration [24].

3. Details of a Simulation Procedure

The processes of homoepitaxial surface growth were studied with the help of numerical simulations. For this purpose, the system of equations (6) was numerically solved on a two-dimensional square $L \times L$ mesh with the linear size $L = 512\ell$ and periodic boundary conditions. The spatial derivatives were calculated in the $\mathbf{r}$-space using a standard finite-difference scheme. For the calculation of the derivative $\nabla M(x)\nabla x$, the following mathematical construction was applied [37]:

$$\nabla_{i,j} M_{i,j}\nabla_{i,j} x_{i,j} = \frac{M_{i+1,j} + M_{i,j}}{2}\frac{x_{i+1,j} - x_{i,j}}{(\Delta x)^2} -$$
$$- \frac{M_{i,j} + M_{i-1,j}}{2}\frac{x_{i,j} - x_{i-1,j}}{(\Delta x)^2} +$$
$$+ \frac{M_{i,j+1} + M_{i,j}}{2}\frac{x_{i,j+1} - x_{i,j}}{(\Delta x)^2} -$$
$$- \frac{M_{i,j} + M_{i,j-1}}{2}\frac{x_{i,j} - x_{i,j-1}}{(\Delta x)^2}, \qquad (7)$$

where the notation $M_{i,j} = M(x_{i,j})$ is used.

The system of equations (6) was integrated with the double-precision accuracy and making use of the Verlet algorithm [37]. The integration steps were equal to $\Delta x = 1.0$ for the spatial coordinate and $\Delta t = 10^{-3}$ for the temporal one, which provided the stability of the selected method [38]. The calculations were carried out till the dimensionless time $t = 10^3$. Hence, in the course of one simulation procedure, each of 524288 equations was solved 10^6 times.

The Gaussian distribution with $\langle\phi(\mathbf{r}, 0)\rangle = 0$ and, taking the nonzero substrate roughness into account, $\langle(\delta\phi)^2\rangle = 0.1$ was chosen as the initial condition for the phase field $\phi(\mathbf{r}, t)$. For the adsorbate concentration field $x(\mathbf{r}, t)$, we put $x(\mathbf{r}, 0) = 0$. The calculations were performed at the fixed values $\varpi^2 = 2$ and $\lambda = 10$ of the parameters that control the phase-field dynamics and at $D_0 = 1$. As was shown in works [25, 30], the growth dynamics of a thin structured film and its morphology under isotropic surface diffusion conditions are mainly governed by the parameters F and ε. In order to study the influence of the anisotropic diffusion with the coefficient D_{em} on the surface growth dynamics and the statistical properties of the surface, we took $F = 2$ and $\varepsilon = 4$. This parameter set corresponds to the case where well-pronounced pyramidal structures of the adsorbate are formed in the course of epitaxial growth in the isotropic case.

4. Results and Their Discussion

The snapshots illustrating a typical evolution of the surface morphology, i.e. the field $\phi(\mathbf{r}, t)$, at fixed time moments t are shown in Fig. 1. They were calculated by simulating the process of homoepitaxial film growth in the absence of an electric field near the substrate (model with the isotropic surface diffusion). Here, the gray color intensity corresponds to the height of the growing surface, which varies from the minimum $\phi_{\min}$ (black color) to the maximum $\phi_{\max}$ (white color).

One can see that in the course of system evolution described by the system of equations (6), the processes of adsorbate self-organization lead from the initial uniform Gaussian distribution of the surface height field, i.e. the order parameter ϕ, to the formation of separate adsorbate islands. Distinct terraces of pyramidal structures are formed at the early stages of the adsorbate structure evolution. Those structures grow in time: their heights and linear sizes become
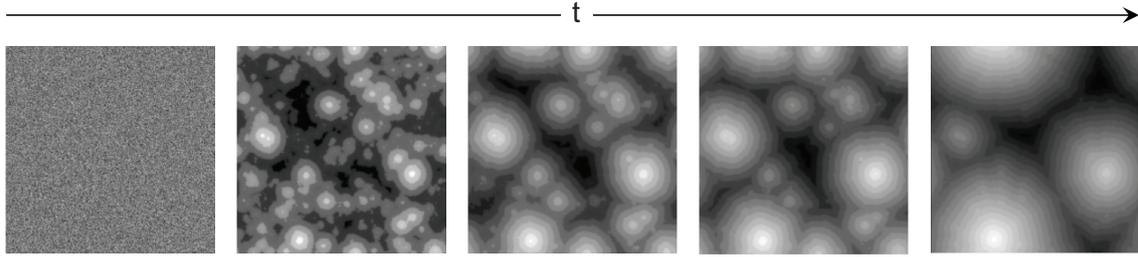
Fig. 1. Typical evolution of the surface morphology at the epitaxial growth in the absence of electromigration effects

larger. If the deposition time is long enough, the adsorbate structures begin to interact with one another so that larger pyramids absorb smaller ones. The finite size of the lattice and the periodic boundary conditions give rise to a single pyramidal structure in the limit of a very long deposition time. It should be noted that, according to the considered model, the minimum value of the phase field, $\phi_{\min}$, increases in time. This circumstance means that both the film thickness and the height of the superficial multilayer structures increase in the course of deposition.

In order to statistically analyze the surface growth process at the deposition [39], let us consider the dynamics of the phase field dispersion (the standard deviation of ϕ)

$$W^2(t) = \left\langle [\phi(\mathbf{r}, t) - \langle \phi(\mathbf{r}, t)\rangle]^2 \right\rangle,$$

the phase field asymmetry

$$m_3 = \frac{\left\langle (\phi(\mathbf{r}) - \langle \phi(\mathbf{r})\rangle)^3 \right\rangle}{(W^2)^{3/2}},$$

and the phase field excess

$$m_4 = \frac{\left\langle (\phi(\mathbf{r}) - \langle \phi(\mathbf{r})\rangle)^4 \right\rangle}{(W^2)^2},$$

where $\langle \phi(\mathbf{r}, t)\rangle$ is the average value of the surface height determined at every time moment t in the standard way,

$$\langle \phi(\mathbf{r}, t)\rangle \equiv L^{-2} \sum_{\mathbf{r}} \phi(\mathbf{r}, t).$$

The dispersion W^2 plays the role of an order parameter for the structuring process. Its increase with time testifies to the presence of ordering processes, i.e. the growth of surface structures. The asymmetry parameter m_3 characterizes the symmetry of the surface

height distribution (the phase field $\phi(\mathbf{r})$) with respect to the average level. In particular, a positive m_3-value means that most points at the surface are located above the average level $\langle \phi(\mathbf{r})\rangle$; if $m_3 < 0$, the majority of the values of the surface height field are smaller than the average value $\langle \phi(\mathbf{r})\rangle$. Finally, the excess parameter m_4 characterizes the randomness of a height distribution and describes the surface stochasticity with respect to the Gaussian surface. For a surface characterized by the Gaussian distribution of heights, we have $m_3 = 0$ and $m_4 = 3$.

The dependences $W^2(t)$ obtained for various values of the electromigration-induced diffusion coefficient D_{em} are depicted in Fig. 2, *a*. One can see that, at the initial stage of epitaxial growth (stage I), the dispersion W^2 does not change in time and has magnitudes of about 10^{-3} for all values of the induced diffusion coefficient D_{em}. At this stage, the adsorbate is accumulated in the first layer. The start of the film growth processes is accompanied by an oscillatory dynamics of $W^2(t)$ as long as $W^2 < 1$ (stage II). The frequency of oscillations is not sensitive to the induced diffusion coefficient. For larger values of the induced diffusion coefficient, the oscillatory dynamics of $W^2(t)$ takes place during longer deposition times. At the next stage (stage III), the value of W^2 increases with time, and the corresponding growth dynamics substantially depends on the anisotropy degree of the adsorbate surface diffusion determined by the parameter D_{em}.

From a comparison between the curves calculated for the isotropic ($D_{em} = 0$, curve *1*) and anisotropic ($D_{em} = 0.5$, curve *2*) cases, it follows that the electromigration-induced anisotropy of the surface diffusion hinders the surface structuring in the course of deposition. An increase of the anisotropic surface diffusion coefficient of the adsorbate stimulated by applying an electric field to the substrate addition-
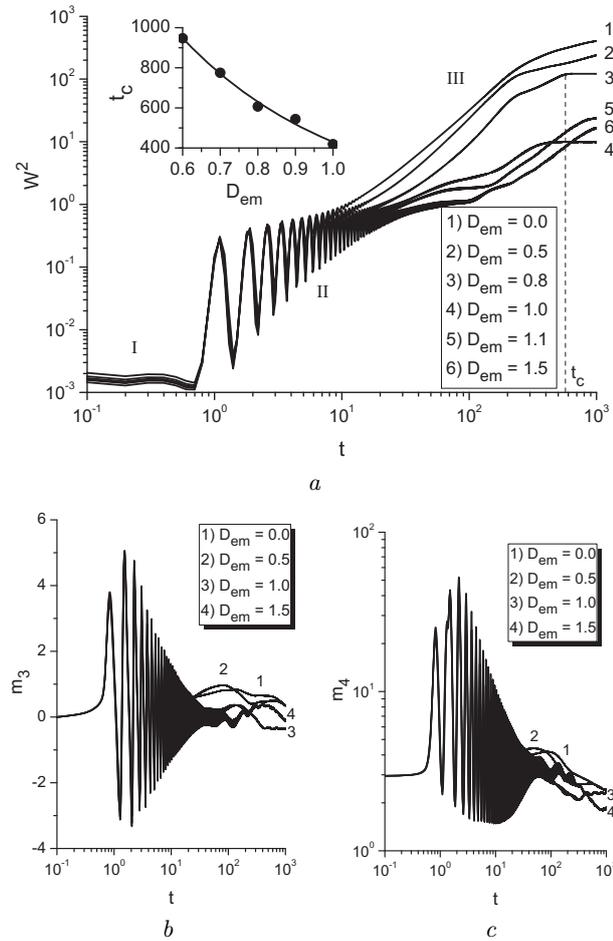
Fig. 2. Time dependences of (a) the dispersion W^2, (b) the asymmetry m_3, and (c) the excess m_4 at various values of the diffusion coefficient D_{em}. The inset in panel (a) demonstrates the dependence of the time t_c required for a stationary regime to be established on the diffusion coefficient D_{em}

ally hinders the surface structuring process and finally leads to the establishment of a stationary regime in the $W^2(t)$-dynamics (see curve 3 calculated for $D_{em} = 0.8$, the section after $t = t_c$). Larger values of the electromigration-induced diffusion coefficient D_{em} give rise to shorter time values t_c (cf. curves 3 and 4 in Fig. 2, a). A more detailed analysis showed that t_c exponentially decreases, as D_{em} increases, which is illustrated by the solid curve in the inset in Fig. 2, a (numerical simulation data are exhibited by circles). If the surface diffusion anisotropy is strong enough, e.g., $D_{em} > 1$, a further increase of D_{em} brings about a slowdown of the $W^2(t)$-dynamics (see curves 5 and 6 in Fig. 2, a).

The evolution dynamics of the asymmetry m_3 and the excess m_4 is shown in Figs. 2, b and 2, c, respectively. At the initial deposition stage, the both parameters acquire the Gaussian values, $m_3 \simeq 0$ and $m_4 \simeq 3$, and this stage corresponds to stage I in the $W^2(t)$-dynamics. The oscillatory dynamics of both quantities (stage II) is characterized by much larger amplitudes as compared with the order-parameter dynamics $W^2(t)$. At the late deposition stage (stage III), both m_3 and m_4 change weakly with time. It should be noted that, for certain values of the anisotropic diffusion coefficient, the both quantities demonstrate a stationary regime (see curves 3 calculated for $D_{em} = 1$). However, the stationary character of the W^2-, m_3-, and m_4-values only testifies to the invariance of the statistical parameters of the growing surface rather than the stationary character of the deposition or film growth processes. The growth dynamics of the film thickness and the surface structure height will be analyzed below.

In order to study, in detail, the hindering of the surface growth dynamics by electromigration effects induced by an external electric field, let us calculate the average time $\langle t \rangle$ required for one thousand atomic layers to grow at various values of the induced diffusion coefficient D_{em}. The results obtained are presented in Fig. 3 as solid circles. It is evident that the average time required for 1000 atomic layers to grow increases with the diffusion coefficient D_{em}. It should be noted that the law describing the dependence $\langle t \rangle$ versus D_{em} changes, when D_{em} exceeds a critical value $D_{em}^c \simeq 0.95$. The numerical results obtained at $D_{em} < D_{em}^c$ can be well approximated by the exponentially growing function $\langle t \rangle = t_1 + a_1 \exp(D_{em}/b_1)$ (the dashed curve in Fig. 3). At $D_{em} > D_{em}^c$, the average time $\langle t \rangle$ increases more slowly with D_{em}, and the numerical results correspond to the logarithmic dependence $\langle t \rangle = t_2 + a_2 \ln(D_{em}/b_2)$ (the solid curve in Fig. 3). The maximum value of the coefficient of determination was a criterion for approximating the obtained numerical data.

Now, let us analyze the growth dynamics of the film thickness and the height of the surface pyramidal structures by varying the induced diffusion coefficient D_{em}. As was mentioned above, both the maximum, $\phi_{\max}$, and minimum, $\phi_{\min}$, values of the phase field ϕ increase in the course of deposition. Therefore, the parameter $d \equiv \phi_{\min}$ can be associated with the thickness of a film consisting of densely packed

adatoms. Then the height of the surface structures is determined as the difference $h \equiv (\phi_{max} - \phi_{min})$. The temporal evolution of the parameters d and h is illustrated in Fig. 4 by the dashed and solid curves, respectively. The exhibited results correspond to the parameter values $(d, h) \geq 1$. The stages of adsorbate rearrangement on the substrate are neglected. Curves *1* were obtained for the isotropic case ($D_{em} = 0$), and curves 2 for the anisotropic one with $D_{em} = 1.5$.

First of all, it should be noted that the electromigration does not affect considerably the law of the film thickness growth, $d(t) \simeq bt$, where the growth rate decreases from $b = 3.04$ at $D_{em} = 0$ to $b = 2.68$ at $D_{em} = 1.5$ (dashed curves *1* and *2*, respectively, in Fig. 4). At the same time, the growth dynamics $h(t)$ of the surface structure height substantially depends on the diffusion coefficient D_{em}. Namely, the growth of D_{em} leads not only to a significant decrease in the surface structure height, but also to the appearance of a certain randomness in the character of the dependence $h(t)$ [cf. curves *1* ($D_{em} = 0$) and *2* ($D_{em} = 1.5$) in Fig. 4].

It should also be noted that the power-law dependence $h(t) \propto t^{\delta}$ is realized for the structure height at the late evolution stage. The analysis of solid curves *1* and *2* shows that the growth index δ depends on the diffusion coefficient D_{em}. The inset in Fig. 4 demonstrates the values of the growth parameter δ for various D_{em} values. One can see that the growth index δ firstly decreases to a certain minimum value at $D_{em} < D_{em}^{c}$ and then begins to increase. Hence, the strengthening of electromigration effects leads, on the one hand, to smaller heights of surface structures and, on the other hand, to a more intensive growth dynamics of structure heights at the late stage. Furthermore, if $D_{em} > D_{em}^{c}$, the growth index does not depend on the induced diffusion coefficient and acquires the value $\delta \simeq 0.46$ (see the inset in Fig. 4).

Now, let us analyze the influence of the diffusion coefficient D_{em} on the average film thickness, $\langle d \rangle$, and the average height of surface structures, $\langle h \rangle$, obtained after a long-term deposition (at $t = 10^{3}$) in the quasistationary regime. The corresponding results are presented in Fig. 5. One can see that if $D_{em} < D_{em}^{c}$, the larger electric field strengths near the substrate lead to narrower film thicknesses and smaller heights of the surface structures. It should be noted that, in this case, the film thickness decreases only by 15%,
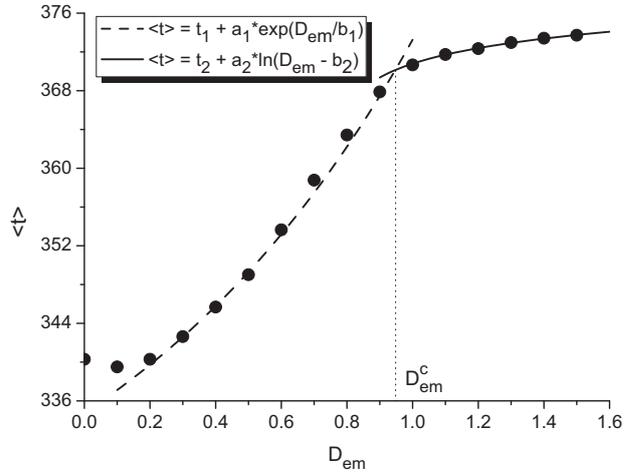
Fig. 3. Dependence of the time $\langle t \rangle$ required for 1000 atomic layers to grow on the diffusion coefficient D_{em}. The parameters of approximation curves are $t_1 = 312.37$, $a_1 = 22.4$, and $b_1 = 1$ (dashed curve); and $t_2 = 374.55$, $a_2 = 2.6$, and $b_2 = 0.76$ (solid curve)
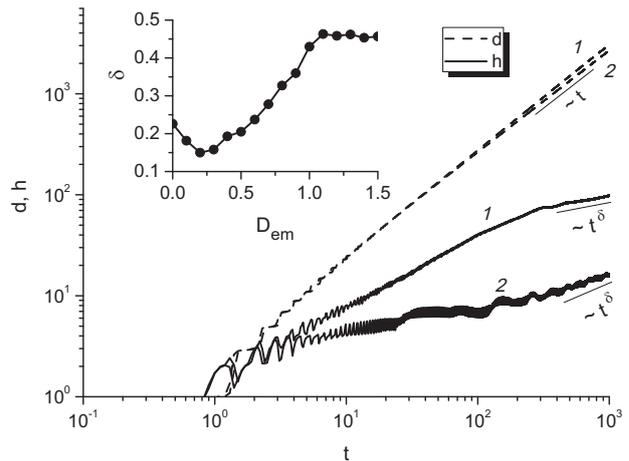
Fig. 4. Time dependences of the film thickness d (dashed curves) and the height of surface structures h (solid curves) for various values of the diffusion coefficient $D_{em} = 0.0$ (curves *1*) and 1.5 (curves *2*). The dependence of the growth index δ on the diffusion coefficient D_{em} in the long-term deposition limit is shown in the inset

whereas the height of surface structures and, accordingly, the number of layers in pyramidal structures decreases considerably with the growth of D_{em}. At the same time, if $D_{em} > D_{em}^{c}$, the electromigration does not substantially affect the $\langle d \rangle$- and $\langle h \rangle$-values. Thus, the electromigration effects destroy the terraces of pyramidal adsorbate structures and favor
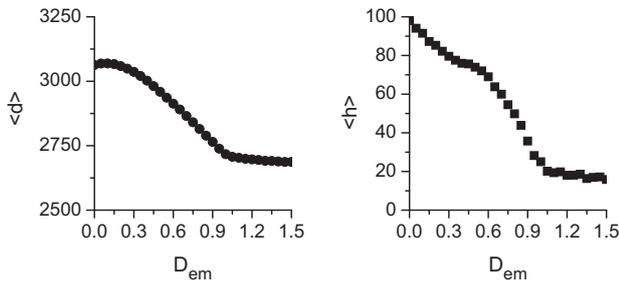
Fig. 5. Dependences of the average film thickness $\langle d \rangle$ (left panel) and the height of surface structures $\langle h \rangle$ (right panel) on the diffusion coefficient D_{em} in the long-term deposition limit ($t = 10^3$)
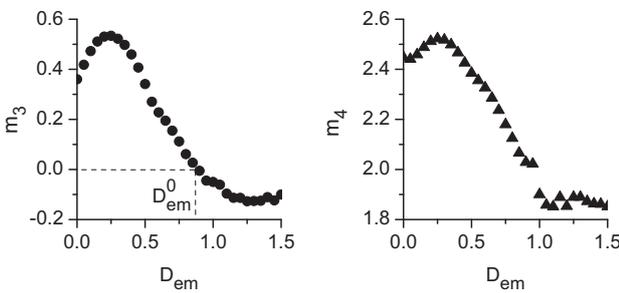
Fig. 6. Dependences of the statistical moments m_3 (left panel) and m_4 (right panel) on the diffusion coefficient D_{em} at $t = 10^3$
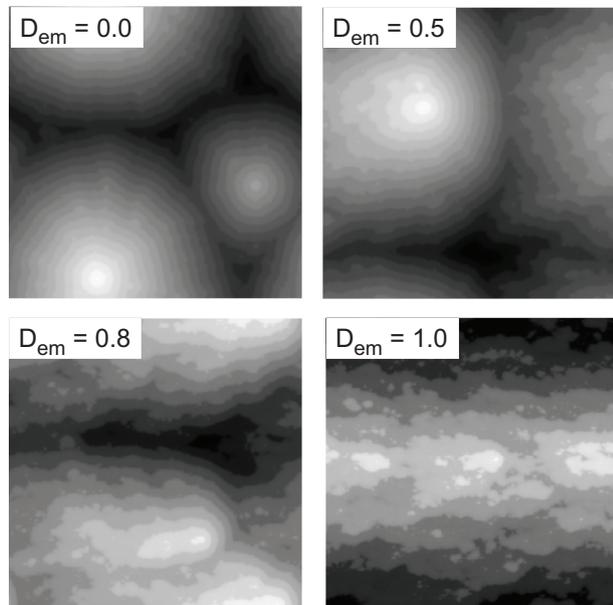
Fig. 7. Typical examples of a surface morphology in the quasistationary regime of film growth at various values of the diffusion coefficient D_{em}
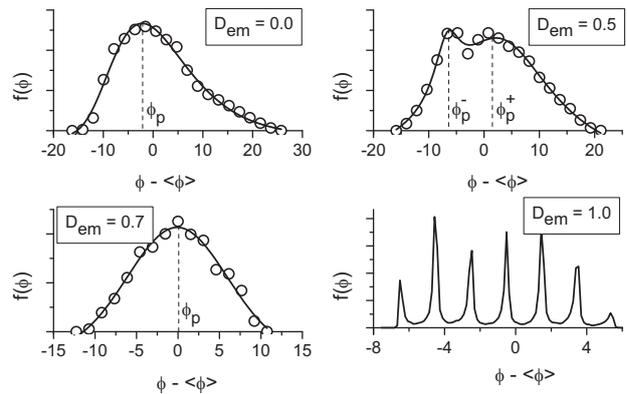
Fig. 8. Distributions of the surface height reckoned from the average value $\langle \phi \rangle$ for the structures shown in Fig. 7

the homogenization of the adsorbate distribution over the film.

To characterize the influence of the electromigration-induced anisotropy of the surface adsorbate diffusion on the surface-height distribution after a long-term deposition, let us analyze the dependences of the asymmetry m_3 and excess m_4 of the surface obtained at $t = 10^3$ on the field-induced diffusion coefficient D_{em}. The calculated dependences $m_3(D_{em})$ and $m_4(D_{em})$ are shown in Fig. 6.

Typical examples of the surface morphology obtained after the long-term evolution ($t = 10^3$) with various values of the diffusion coefficient D_{em} are exhibited in Fig. 7. The calculated distributions of the height fields over their values are presented in Fig. 8. The analysis of the obtained results testifies that if the diffusion is isotropic ($D_{em} = 0$), the surface is characterized by the values $m_3 > 0$ and $m_4 < 3$. This means that the surface is statistically different from Gaussian. Namely, the height distribution is asymmetric and the majority of surface height values exceed the average value. The height field distribution calculated for $D_{em} = 0.0$ is given in Fig. 8. The numerical data are exhibited by hollow circles. They agree well with the Generalized Extreme Value Distribution, which looks like [40]

$$f(\phi) = \kappa^{-1} \exp\left(-z\right) \exp\left\{-\exp\left(-z\right)\right\},$$

where $z \equiv (\phi - \mu)/\kappa$, and μ and κ are approximation parameters. This distribution is evidently asymmetric, and most of the ϕ-field values are larger than the mean value $\langle \phi \rangle$. At the same time, for the most probable value ϕ_p, we have $\phi_p < \langle \phi \rangle$. The deviation

of m_4 from a value of 3 typical of the Gaussian distribution (see Fig. 6) testifies to the spatial ordering of adsorbates on the surface, with the implementation of terraces in the spatial distribution of heights, which is different from the case of the Gaussian random field.

With the growth of the induced diffusion coefficient D_{em}, the values of both statistical quantities m_3 and m_4 become somewhat larger, achieve corresponding maximum values, and afterward decrease to corresponding fixed values, with the asymmetry parameter changing its sign at $D_{em} = D_{em}^0$. Hence, the enlargement of D_{em} leads to a morphological transformation of the surface structure from a surface with the majority of height values exceeding the average value to a surface with the overwhelming majority of height values being smaller than the average value. In this case, a decrease of the excess value m_4 with the growth of D_{em} testifies to an increase of correlations along the surface and, as a result, an increase of the width of terraces in the surface structures.

At $D_{em} = 0.5$, the surface adsorbate structures are characterized by the electromigration-induced anisotropy in the direction of the electric field applied to the substrate (see Fig. 7). In this case, the surface height distribution becomes more symmetric and has two main peaks: at $\phi = \phi_p^- < \langle\phi\rangle$ and $\phi = \phi_p^+ > \langle\phi\rangle$ (see the $D_{em} = 0.5$-distribution in Fig. 8). The corresponding numerical data are approximated well by a superposition of two Gaussians.

If the induced diffusion coefficient increases further, the surface structures become elongated along the field applied to the substrate (see the $D_{em} = 0.8$-example of the surface morphology in Fig. 7). It should be noted that, in the case $D_{em} \simeq 0.8$, we have $m_3 = 0$ (see Fig. 6), which means a symmetric distribution of surface height values with respect to the average value $\langle\phi\rangle$ [see panel $D_{em} = 0.8$ in Fig. 8; the solid curve is the approximation of numerical data (hollow circles) by a single-mode Gaussian, for which $\phi_p \simeq \langle\phi\rangle$].

At even higher values of the induced diffusion coefficient, $D_{em} > D_{em}^c$, both the asymmetry and excess parameters do not depend substantially on D_{em} (see Fig. 6). Under such growing conditions, the applied electric field leads to the destruction of well-pronounced surface pyramidal structures. In this case, a single percolating cluster of the adsorbate is formed, which possesses a small number of wide terraces with non-smooth boundaries (see the $D_{em} = 1.0$-snapshot in Fig. 7). The corresponding surface differs substantially from the Gaussian one, being characterized by the excess value $m_4 \simeq 1.85$ (see Fig. 6). The asymmetry value $m_3 \simeq -0.15$ testifies that the majority of the height field values are smaller than the average value, but this majority is not considerable. The corresponding height distribution calculated in the case $D_{em} = 1.0$ is shown in the $D_{em} = 1.0$-panel in Fig. 8. It demonstrates the presence of a small number of terraces (the number of peaks is equivalent to the number of terraces).

5. Conclusions

In this work, the influence of electromigration effects on the dynamics of epitaxial growth of thin films is studied in the framework of the phase-field theory and using the numerical simulation procedure. The electromigration effects are taken into account by introducing a directed flux of adatoms with the diffusion coefficient proportional to the strength of the electric field applied to the substrate.

It is found that an increase of the induced diffusion coefficient leads to a slowdown of the growth dynamics for both the film thickness and the height of the surface multilayer adsorbate structures, as well as to the symmetry of the height field distribution over its values. It is shown that the electromigration effects lead to the formation of anisotropic surface structures. At the coarsening stage, the growth dynamics of structure heights is given by a power law. The corresponding growth index increases to a stationary value of about 0.46, as the induced diffusion coefficient increases to a certain critical value. At large induced diffusion coefficient values, the process of epitaxial growth gives rise to the formation of a multilayer percolating structure of the adsorbate with wide terraces characterized by non-smooth boundaries. If the coefficient of induced diffusion exceeds the critical value, the dynamics of surface growth and its statistical properties do not depend substantially on the electric field strength.

The results obtained in this work can be useful for predicting the dynamics of epitaxial film growth in the presence of an electric field near the substrate and for correcting the technological conditions while growing surface structures with a required morphology.

1. J.R. Black. Electromigration – A brief survey and some recent results. *IEEE Trans. Electr. Dev.* **16**, 338 (1969).

2. P.S. Ho, T. Kwok. Electromigration in metals. *Rep. Prog. Phys.* **52**, 301 (1989).

3. Y. Homma, R.J. Mcclelland, H. Hibino. DC-resistive-heating-induced step bunching on vicinal Si (111). *Jap. J. Appl. Phys.* **29**, L2254 (1990).

4. E.D. Williams, E. Fu, Y.N. Yang *et al.* Measurement of the anisotropy ratio during current-induced step bunching. *Surf. Sci.* **336**, L746 (1995).

5. B.J. Gibbons, J. Noffsinger, J.P. Pelz. Influence of Si deposition on the electromigration induced step bunching instability on Si(111). *Surf. Sci.* **575**, L51 (2005).

6. S. Lin, Y. Liu, S. Chiu *et al.* The electromigration effect revisited: non-uniform local tensile stress-driven diffusion. *Sci. Rep.* **7**, 3082 (2017).

7. F. Leroy, D. Karashanova, M. Dufay *et al.* Step bunching to step-meandering transition induced by electromigration on Si(111) vicinal surface. *Surf. Sci.* **603**, 507 (2009).

8. V. Usov, C.O. Coileain, I.V. Shvets. Influence of electromigration field on the step bunching process on Si(111). *Phys. Rev. B* **82**, 153301 (2010).

9. O. Toktarbaiuly, V. Usov, C.O. Coileain *et al.* Step bunching with both directions of the current: Vicinal W(110) surfaces versus atomistic-scale model. *Phys. Rev. B* **97** 035436 (2018).

10. A.A. Shklyaev, A.V. Latyshev. Electromigration effect on the surface morphology during the Ge deposition on Si(111) at high temperatures. *Appl. Surf. Sci.* **465**, 10 (2019).

11. B. Voigtlander. Fundamental processes in Si/Si and Ge/Si epitaxy studied by scanning tunneling microscopy during growth. *Surf. Sci. Rep.* **43**, 127 (2001).

12. A.A. Shklyaev, M. Ichikawa. Extremely dense arrays of germanium and silicon nanostructures. *Phys. Usp.* **51**, 133 (2008).

13. A.A. Shklyaev, K.N. Romanyuk, S.S. Kosolobov. Surface morphology of Ge layers epitaxially grown on bare and oxidized Si(001) and Si(111) substrates. *Surf. Sci.* **625**, 50 (2014).

14. S.A. Teys. Different growth mechanisms of Ge by Stranski-Krastanow on Si (111) and (001) surfaces: An STM study. *Appl. Surf. Sci.* **392**, 1017 (2017).

15. J.M. MacLeod, J.A. Lipton-Duffin, U. Lanke *et al.* Shape transition in very large germanium islands on Si(111). *Appl. Phys. Lett.* **94**, 103109 (2009).

16. A. Shklyaev, L. Bolotov, V. Poborchii *et al.* Properties of three-dimensional structures prepared by Ge dewetting from Si(111) at high temperatures. *J. Appl. Phys.* **117**, 205303 (2015).

17. A. Voigt. *Multiscale Modeling in Epitaxial Growth* (Birkhäuser, 2000) [ISBN: 3-7643-7208-7].

18. C. Ratsch, P. Puggerone, M. Scheffler. *Surface Diffusion: Atomistic and Collective Processes* (Plenum, 1997) [ISBN: 978-1-4899-0262-7].

19. H. Metiu, Y.-T. Lu, Z.Y. Zhang. Epitaxial growth and the art of computer simulations. *Science* **255**, 1088 (1992).

20. C. Ratsch, M.F. Gyure, R.E. Caflisch *et al.* Level-set method for island dynamics in epitaxial growth. *Phys. Rev. B* **65**, 195403 (2002).

21. S. Park, H. Jeong, B. Kahng. Numerical test of the damping time of layer-by-layer growth on stochastic models. *Phys. Rev. E* **59**, 6184 (1999).

22. D.O. Kharchenko, V.O. Kharchenko, I.O. Lysenko *et al.* Stochastic effects at ripple formation processes in anisotropic systems with multiplicative noise. *Phys. Rev. E* **82**, 061108 (2010).

23. F. Liu, H. Metiu. Stability and kinetics of step motion on crystal surfaces. *Phys. Rev. E* **49**, 2601 (1994).

24. A. Karma, M. Plapp. Spiral surface growth without desorption. *Phys. Rev. Lett.* **81**, 4444 (1998).

25. V.O. Kharchenko, D.O. Kharchenko, A.V. Dvornichenko. Scaling properties of pyramidal islands formation process at epitaxial growth. *Eur. Phys. J. B* **88**, 3 (2015).

26. D. Kandel, E. Kaxiras. Microscopic theory of electromigration on semiconductor surfaces. *Phys. Rev. Lett.* **76**, 1114 (1996).

27. S. Stoyanov, V. Tonchev. Properties and dynamic interaction of step density waves at a crystal surface during electromigration affected sublimation. *Phys. Rev. B* **58**, 1590 (1998).

28. V. Popkov, J. Krug. Dynamic phase transitions in electromigration-induced step bunching. *Phys. Rev. B* **73**, 235430 (2006).

29. B. Ranguelov, S. Stoyanov. Instability of vicinal crystal surfaces with transparent steps: Transient kinetics and non-local electromigration. *Surf. Sci.* **603**, 2907linebreak (2009).

30. D.O. Kharchenko, V.O. Kharchenko, I.O. Lysenko. Phase-field modeling of epitaxial growth in stochastic systems with interacting adsorbate. *Phys. Scr.* **83**, 045802 (2011).

31. D.O. Kharchenko, V.O. Kharchenko, T. Zhylenko *et al.* A study of pyramidal islands formation in epitaxy within the generalized phase-field model. *Eur. Phys. J. B* **86**, 175 (2013).

32. V.O. Kharchenko, D.O. Kharchenko. Nanosize structure formation in overdamped stochastic reaction-diffusion systems with interacting adsorbate. *Phys. Rev. E* **86**, 041143 (2012).

33. V.O. Kharchenko, D.O. Kharchenko, S.V. Kokhan *et al.* Properties of nano-islands formation in nonequilibrium reaction-diffusion systems with memory effects. *Phys. Scr.* **86**, 055401 (2012).

34. V.O. Kharchenko, D.O. Kharchenko, A.V. Dvornichenko. Statistical properties of nanosized clusters on a surface in overdamped stochastic reaction-Cattaneo systems. *Surf. Sci.* **630**, 158 (2014).

35. V.O. Kharchenko, D.O. Kharchenko. Noise-induced structure formation in system of point defects subjected to irradiation. *Eur. Phys. J. B* **85**, 383 (2012).

36. V.O. Kharchenko, D.O. Kharchenko. Abnormal grain growth in nonequilibrium systems: Effects of point defect structureing. *Phys. Rev. E* **89**, 042133 (2014).

37. F. Cucker, P.G. Ciarlet. *Handbook of Numerical Analysis. Vol. 11. Special Volume: Foundations of Computational Mathematics* (Amsterdam, 2003) [ISBN: 9780444512475].

38. G. Strang. *Introduction to Applied Mathematics* (Wellesley-Cambridge Press, 1986) [ISBN: 978-0961408800].

39. E.S. Gadelmawla, M.M. Koura, T.M.A. Maksoud *et al.* Roughness parameters. *J. Mater. Process. Tech.* **123**, 133 (2002).

40. G. Muraleedharan, C.G. Soares, C. Lucas. Characteristic and moment generating functions of generalised extreme value distribution (GeV). In: *Sea Level Rise, Coastal Engineering, Shorelines and Tides.* Edited by L.L. Wright (Nova Science Publishers, 2009), p. 269 [ISBN 978-1-61728-655-1].

А.В. Дворниченко

ЕФЕКТИ ЕЛЕКТРОМІГРАЦІЇ
ПРИ ЕПІТАКСІАЛЬНОМУ РОСТІ ТОНКИХ ПЛІВОК:
МОДЕЛЮВАННЯ МЕТОДОМ ФАЗОВОГО ПОЛЯ

У роботі проводиться теоретичне дослідження процесу росту тонких плівок при епітаксії з урахуванням анізотропії поверхневої дифузії адсорбату, індукованої ефектами електроміграції, в рамках теорії фазового поля з використанням процедури числового моделювання. Встановлено вплив коефіцієнта індукованої анізотропної дифузії, пропорційного до напруженості підведеного електричного поля, на динаміку росту товщини плівки та висоти поверхневих структур, морфологію зростаючої поверхні, статистичні властивості поверхневих багатошарових структур адсорбату та розподіл поверхневих структур за висотою.

Ключові слова: метод фазового поля, епітаксіальний ріст, поверхневі структури, електроміграція, числові симуляції, статистичні властивості.